Chapter 7

Fluorescent dye induced wetting of liquid crystal domains at the air-water interface

7.1 Introduction

Interesting and rich phenomenology has been observed at interfaces between solid-liquid and liquid-gas in a variety of systems [1, 2, 3]. Currently, wetting-dewetting and roughness correlations have drawn considerable attention due to their scientific importance and technological applications [4]. Droplet spreading over a surface plays an important role in many industrial processes. e.g., ink drying on paper, ink jet printers, xerox, lubrication, drying of paints, spreading of pesticides over a leaf and coating of solids.

For an isotropic liquid deposited on a substrate, at equilibrium, the forces acting on it are given by Young's equation.

$$\gamma_{sg} = \gamma_{sl} + \gamma_{lg} cos(\theta) \tag{7.1}$$

where, γ_{sg} is the surface tension between solid and gas, γ_{sl} is the surface tension between the solid and the liquid, γ_{lg} is the surface tension between the gas and the liquid and θ is the equilibrium contact angle of the drop made with the substrate. Three different regimes of wetting of a domain on solid can be identified. They are, partial wetting(θ varies between 0° and 90°, complete wetting(θ=0°) and non-wetting(θ greater than 90°). For an isotropic liquid, the spreading coefficient, S, is defined as,

$$S = \gamma_{sg} - \gamma_{sl} - \gamma_{lg} \tag{7.2}$$

A positive value of S implies that the spreading is energetically favored and negative value of S indicates partially wetting or dewetting. It has been clearly established now that spreading mechanism lies in the development of a precursor film ahead of the macroscopic domain boundary [5]. The formation of the precursor film was due to a gas phase(for volatile liquid) or diffusion(for non-volatile liquid). Recent experiments indicate that the precursor-film has a thickness of about a molecule. Even at the final stage of spreading the precursor film remains.

Liquid crystals are complex fluids with different order and possess very intricate hydrodynamics. Wetting of anisotropic liquids like liquid crystals(LC) are more interesting and rich in physics. Recent studies on their wetting nature over the substrate indicates it dependency on the mesophase [6]. Reports on smectic liquid crystal(8CB) spreading on a substrate have been analyzed using ellipsometry and xray reflectivity techniques [7, 8], [4]. The major findings from these experiments were the formation of prewetting film during spreading in smectic and nematic phases. The prewetting film was made up of a monolayer and a thick bilayer on top of it. A report on a liquid crystal domain over Silica substrates indicate that the spreading kinetics and wetting behavior depends on the nature of mesophase and has led to different length and time scales. Using scanning polarization force microscopy(non-invasive probe), the layer by layer spreading of 8CB was observed. The 8CB liquid crystal formed domains and pancakes on the surface in smectic phase, wets the surface in nematic and dewets in isotropic phase [9].

Gradients in surface tension can be created within a domain by setting up a gradient in temperature(thermo capillary) or in concentration(diffuso capillary) or electric charges(electro capillary) [10, 11]. Such gradients in surface tension which leads to the flow and are known as *Marangoni effect* [12, 13]. Here, the region of higher surface tension pulls the region of lower surface tension. e.g., Camphor dance, propulsion of soap coated match stick in clean water and the tears in the wine glass.

Insoluble surfactants influence the drop deformation by different mechanisms like surface dilution and Marangoni stresses [14, 15, 16, 17]. In the surface dilution mechanism, increase

of drop area when deformed, dilutes the surfactant concentration. This leads to increase in the interfacial tension which in turn decreases the deformation from that expected for equilibrium surface tension. Marangoni stresses arise from the interfacial tension gradient generated by the convection. These stresses retard the surface flow and consequently increase the deformation. The parameters that govern the deformation of the drop are the shear rate, drop radius, viscosity of the suspending medium and the equilibrium interfacial tension [18].

A spontaneous movement of reactive domains on surfaces with different wetting properties has been reported [19]. Here the domains have velocities in the range 1 mm/sec to 10 cm/sec. A study of surfactant induced marangoni motion of a domain into an external liquid medium shows that asymmetric adsorption of the surfactant at one side of the domain propels it to the medium at higher surface tension [20]. An earlier study on a dopant of liquid crystal with a volatile compound, lead to different boundary conditions at the liquid crystal-substrate interface leading to pattern formation [21]. Here, the interfacial tensions acting at the interfaces changes the boundary conditions as the volatile compound evaporates.

In this chapter, we have investigated the spreading of fluorescent dye doped liquid crystal domains at the air-water(A-W) interface. An amphiphilic fluorescent dye, 4-(hexadecylamino)-7-nitrobenz-2oxa-1,3 diazole(NBDHDA), was used in the experiment. This disperses easily in a liquid crystal host. Here, the irreversible photobleaching of the fluorescent dye causes a gradient in surface tension resulting in the flow of liquid crystalline material. Also, the local heating due to the excitation of dye may cause a temperature gradient and giving rise to a surface tension gradient which may facilitate the flow in LC domains.

7.2 Experiment

The materials n-alkylcyanobiphenyls(Aldrich) were obtained commercially with n=5, 7 and 8. The LC material, octylcyanobiphenyl(8CB), exhibits a smectic phase at room temperature. The LC material, heptylcyanobiphenyl(7CB), exhibits a nematic phase at room temperature. The LC material hexylcyanobiphenyl(6CB), exhibits an isotropic phase at room temperature. These were used for the experiments at the A-W interface. The fluorescent dye NBD-

HDA(Molecular Probes) of 1% to 5% molar concentrations were added as a dopant to the liquid crystal dissolved in chloroform(HPLC grade). The resulting solution was added in excess over a cleaned petri dish filled with Millipore Milli-Q(specific resistance > 18 MΩ-cm) water to form multilayers or lens shaped liquid crystal(LC) domains. This is shown in Figure 7.1. The water level was maintained quite low to prevent the fast drift of the domains. To reduce the drift further, the petri dish was covered with a glass cap. All the experiments were carried out at room temperature(26 °C). A sufficiently big LC domain was tracked in the field

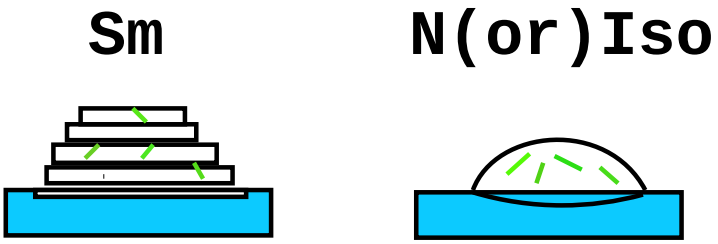

Figure 7.1: Schematic diagram of smectic domains(Sm) and nematic or isotropic domains(N or Iso) doped with fluorescent dye at air-water interface.

of view of the microscope. The excitation of the fluorescent dye was around 450 *nm* and the emission was around 530 *nm*. Appropriate dichroic filters were used for the excitation of the fluorophore. The Leitz Metalux 3 microscope which was modified to have polarizing mode along with epifluorescence and reflection was used to image the thicker LC domains at A-W interface(Figure 7.2). A Hg(100 W) lamp was used as a source. A DXC-390P Sony CCD camera was used for obtaining the images.

The composite signal was sent to PCI-1411(National Instruments) frame grabber which captured the images at a rate of 25 frames/sec. A program written in LabView(software) was used to stored the images continuously at the desired time interval. The images were processed and analysed using the NIH(public domain) and Matlab softwares. The RGB image was converted to 8 bit grey scale image for processing to get the diameter of the domains. To calculate the fluorescent intensity in the domain, we drew a strip over the domains and averaged out the pixels which gave the intensity. We thus monitored the intensity of the LC domains.

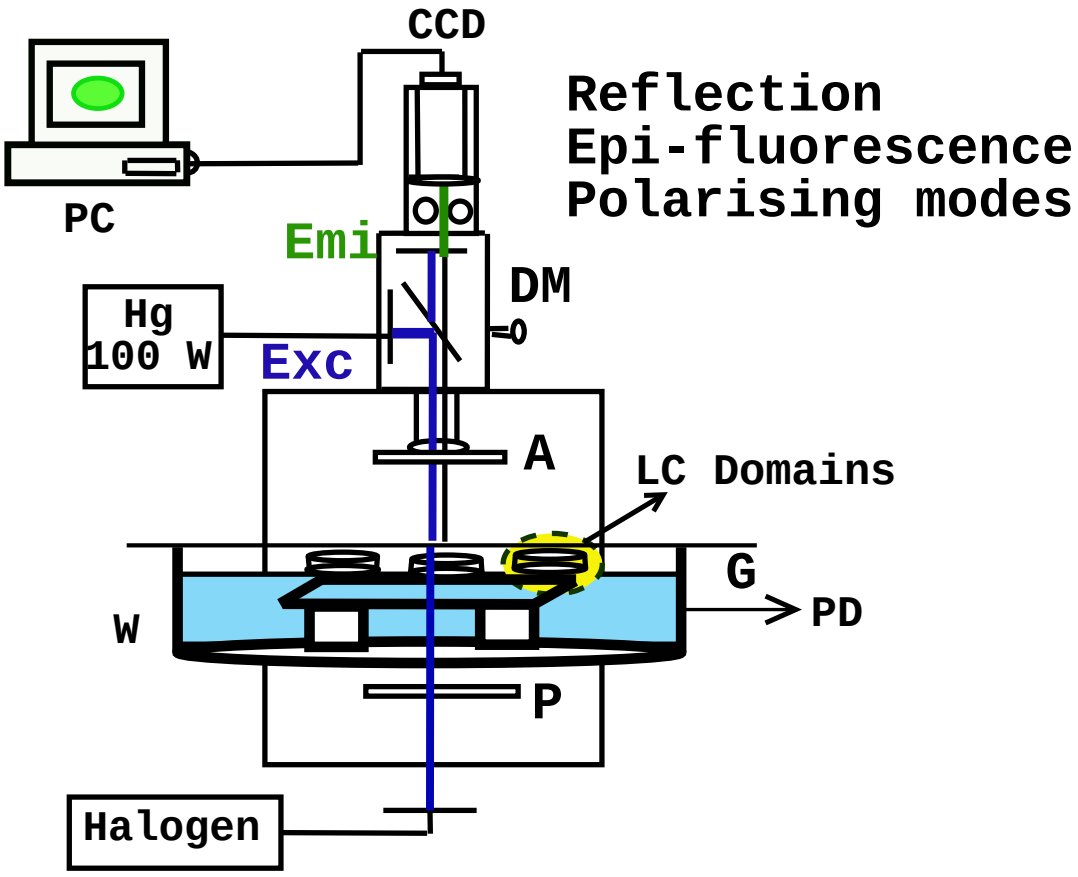

Figure 7.2: Schematic diagram of the microscopy setup for the observation of liquid crystal domains. In this setup, one can observe the thicker LC domains through epifluorescence, reflection and polarising modes. Interchangeable lamps(Halogen and Hg) were used in the experiments. The symbols represent, liquid crystal domains(LC), water(W), petridish(PD), Mercury(Hg) and Halogen lamps, dichroic mirror(DM) and filters(Exc and Emi), glass cap(G), polariser(P), analyser(A), charge coupled device(CCD) and computer(PC).

7.3 Results and Discussions

In reflection mode, we have observed 8CB material doped with 1% fluorescent at A-W interface. Due to interference we find uniform color within the smectic multilayer domains. This indicated an optically flat smectic domains at A-W interface. For nematic and isotropic domains, we observed Newton's rings which indicated that the domains were of lens shaped. These observations are in accordance with other reports [22].

Under epifluorescence, for smectic liquid crystal domains, we observed a variation in the intensities of the domains. This indicated multilayer domains of different thickness. On increasing the intensity of the exciting light of appropriate wavelength, we find in the smec-

tic domains a decrease in the fluorescent intensity. This photobleaching of the fluorescent dye within the LC domains leads to interesting effects. We find in the smectic domain, the photobleaching led to the asymmetric change in the domain diameter. The domain size increases with time. Figure 7.3 shows the evolution of smectic domain as a function of time. The size of smectic domain varies with time. Here, we find that within a domain, the central region has less intensity compared to its periphery. Shearing between the layers was found to occur in smectic during the process of illumination. Under reflection, to begin with, the domain was circular(Figure 7.3(a)). Under epifluorescence, we find the shearing within the domain and flow of layers(Figures 7.3(b) to 7.3(g)). Further illumination leads to merging of the sheared layers giving rise to bigger circular domains(Figure 7.3(h)). At this stage, switching over from epifluorescence to reflection, shows a decrease in diameter of smectic domains. We infer that the decrease in the diameter is due to the increase in the thickness of the domain. This sequence is shown in Figures (7.3(i) to 7.3(l)). This process of thickening of smectic domain was accompanied by the dislocation fronts which started mostly from the periphery and later covered the entire domain. We tracked and plotted the displacement of the dislocation front evolution in time. This is shown in Figure 7.4. It shows a linear dependence in time. The velocity of the front in most cases was around 7.5 μm/sec. However, there was one exception which showed a value of 22 μm/sec. This velocity distribution is very likely dependent on the distribution of the dye concentration in the smectic domain. The presence of dislocation fronts in smectic liquid crystals were reported for the free standing films in equilibrium with its meniscus [23, 24]. Studies on the kinetics of layer thinning transitions on the overheated smectic free standing films were found to nucleate dislocation loops. Here, a linear dependency of the displacement of the dislocation front with time has been reported [25].

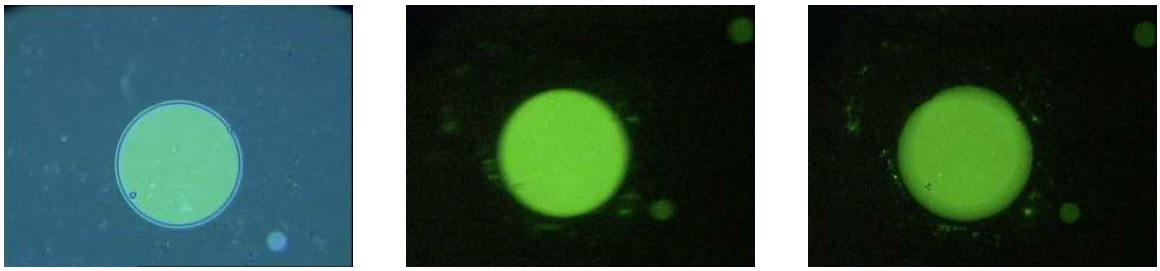

(a) 0 (b) 5 (c) 6

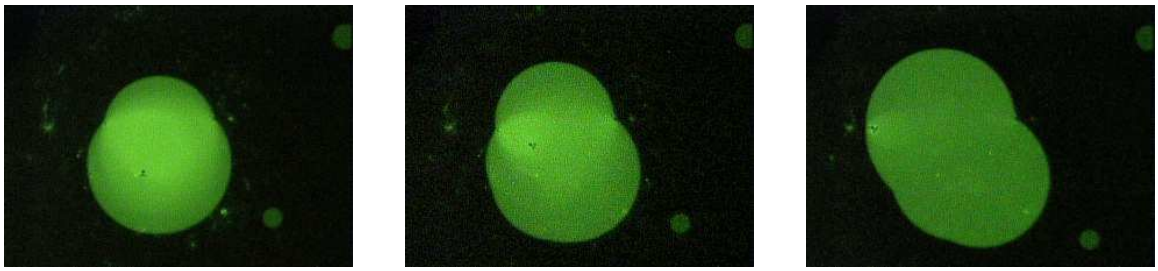

(d) 7 (e) 8 (f) 11

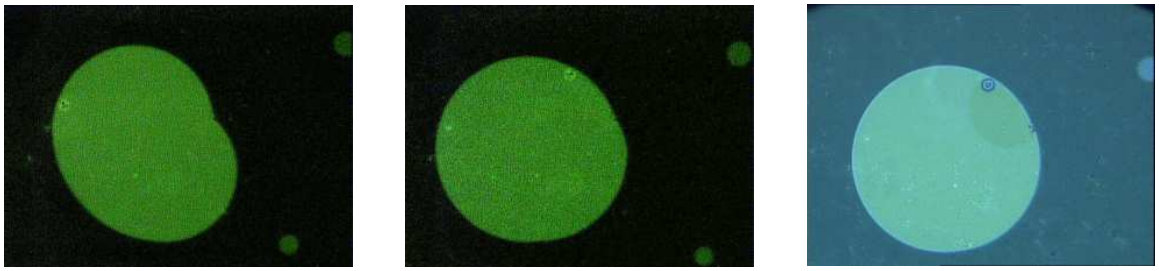

(g) 13 (h) 19 (i) 22

(j) 30 (k) 40 (l) 80

Figure 7.3: Microscopy images showing the evolution of the smectic domain doped with fluorescent dye as a function of time. Figure(a) represents the initial image taken under reflection. Figures (b) to (h) were taken under epifluorescence. Here, the diameter of smectic domains increased due to the movement of the layer. Figures (i) to (l) were taken under reflection where a decrease in diameter due to the movement of dislocation fronts. Scale of each image is 190 x 140 μm^2.

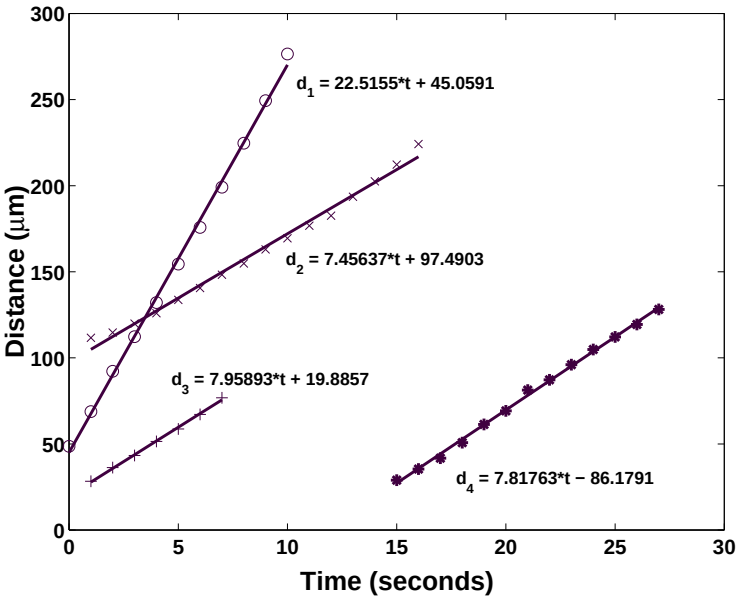

Figure 7.4: Variation of the displacement of the dislocation front with time. The symbols represent the experimental points for different fronts and the continuous lines shows the least square fit. The slope of the fit gives the velocity of the dislocation front.

Figure 7.5(a) shows the initial state of smectic domain under reflection. These domains in some cases, under epifluorescence, develop lobes on the sides during the expansion(Figure 7.5(b)). Again under reflection the domains recover the circular shape accompanied by the dislocation fronts(Figure 7.5(c)). One can repeatedly do this process till the fluorescent dye gets completely bleached.

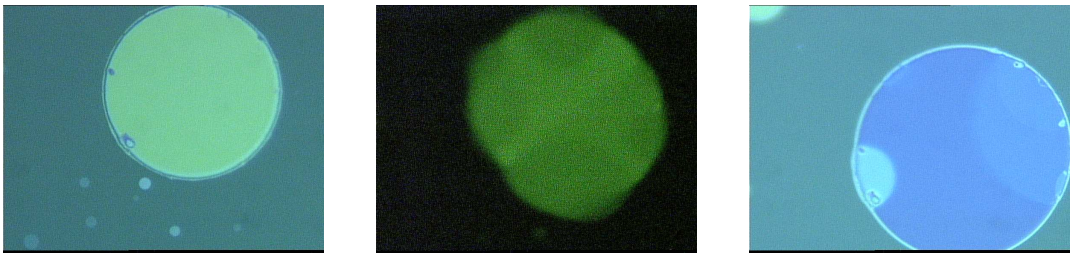

(a) (b) (c)

Figure 7.5: Evolution of smectic domains during photobleaching. Figure(a) shows under reflection the smectic domain in the initial state. Figure(b) shows under epifluorescence the expansion of the domain by the development of side lobes. Figure(c) shows under reflection the reverse process by means of dislocation fronts. Scale of each image is 190 x 140 μm^2.

In a 7CB domain exhibiting nematic phase, we find an uniform expansion of the circu-

lar domains during excitation of the fluorescent dye. This evolution is shown in Figure 7.6. Under reflection the diameter of the domains decreases. The interference rings seen in the nematic domain moved to the periphery during excitation indicating a decrease in the curvature. Under reflection, the interference rings moved towards the center indicating an increase in the curvature of the nematic domains. The variation of the diameter of the domains during the excitation of the dye in epifluorescence and the reflection modes as a function of time is shown in Figure 7.7. Here, the variation of the domain size(ΔD_n), is expressed in percentage. It is given by the ratio of the absolute value of the difference between the final diameter, D_f, and the initial diameter, D_{ini}, to the D_f, i.e. $\Delta\ D_n = (D_f - D_{ini}/D_{ini})$ x 100. We find that the rate of increase in the diameter of the domains was more rapid under epifluorescence compared to the rate of decrease in diameter under reflection. We have determined the decay in fluorescent intensity of the domains. This is shown in Figure 7.8. The decay is rapid in the beginning and later saturates with time. Based on the fits we determine the kinetics of photobleaching within the LC domains at the A-W interface yielding a value of about 0.25 seconds.

We have carried out the experiments with dye concentration upto 5% in 7CB. At higher concentrations of the dye, the domains break into smaller drops and the process is irreversible. This effect was not seen for the LC domains without the fluorescent dye. We find the LC domains to be stable even for prolong illumination. We also carried out the experiments to test on dye doped liquid crystals on an untreated ITO substrate and hydrophilically (Poly-vinyl alcohol) treated substrate. We did not find any change in size of LC domains or any other deformation under epifluorescence and reflection. We attribute this to the strong pinning of the contact line of the liquid crystal domains by the surface heterogeneities, micro scale roughness and chemical affinity which has prevented the LC domain from spreading. However, under the polarising microscope, we could melt the whole nematic domain by increasing the intensity of Hg lamp. We have also studied the effect of illumination under epifluorescence on a free standing dye doped smectic LC film. Here, the surfaces of the film are free and the edges are bounded to the walls. In these experiments, we did not find any

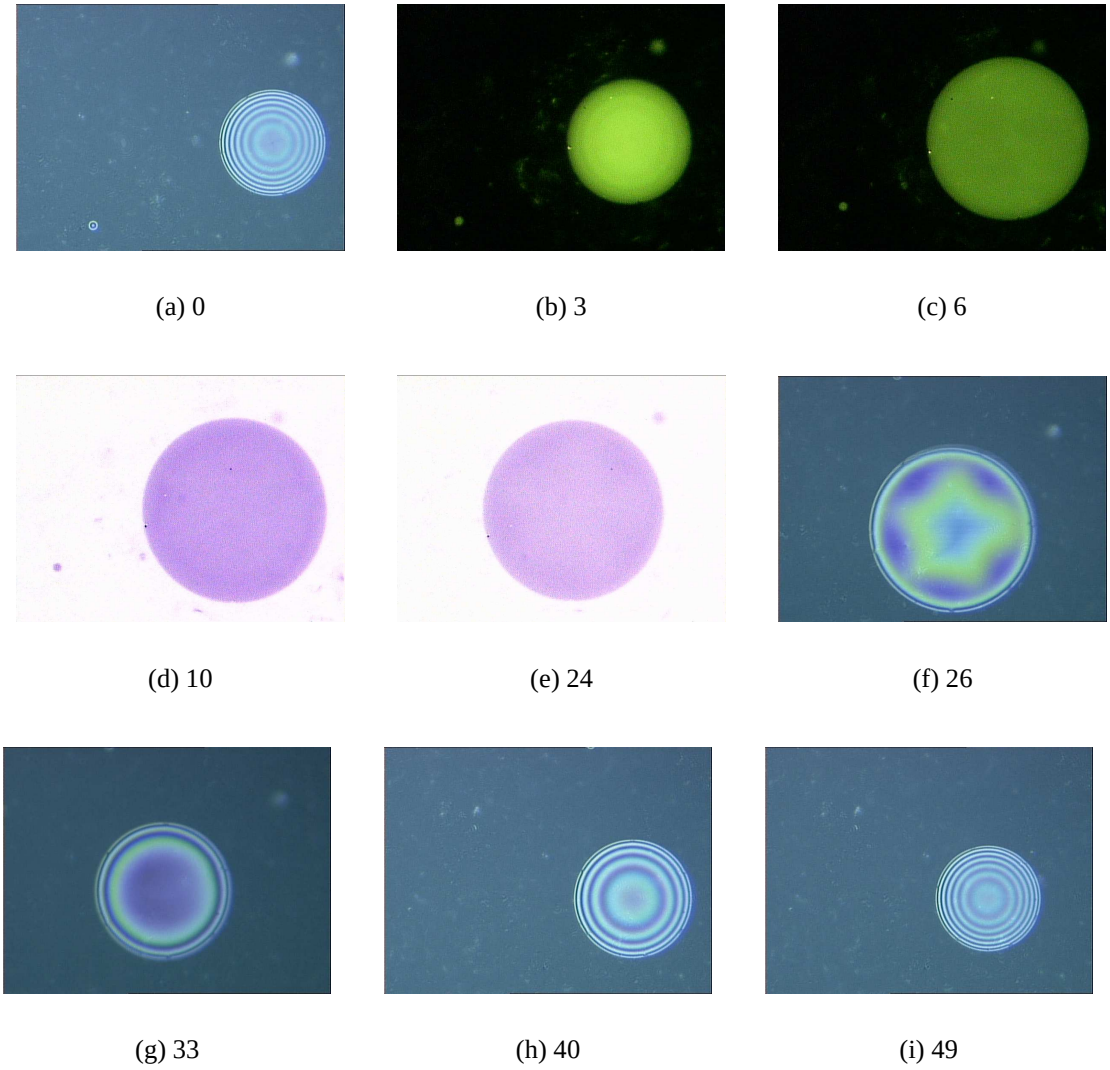

(a) 0 (b) 3 (c) 6

(d) 10 (e) 24 (f) 26

(g) 33 (h) 40 (i) 49

Figure 7.6: Microscopy images showing the evolution of the nematic domain doped with fluorescent dye as a function of time. The time in seconds are given below each image. Figure(a) shows under reflection, the interference Newton's rings of a nematic domain. Figures (b) and (c) show under epifluorescence an uniform increase in diameter of the domain. Figures (d) and (e) show under epifluorescence, further increase in diameter(Here, due to low fluorescence intensity the images which were dull were inverted for better clarity). The nematic domains increased in diameter and became more flattened during excitation. Figures (g) to (i) show under reflection, a decrease in diameter and the reappearance of Newton's rings. Scale of each image is 190 x 140 μm^2.

change in the film sizes and topology. These experiments indicate the effect of dye induced spreading occurs only in LC domains at the smooth A-W interface. This is very likely due to weak anchoring of the LC domains at the A-W interface which is affected by the surfactant impurities.

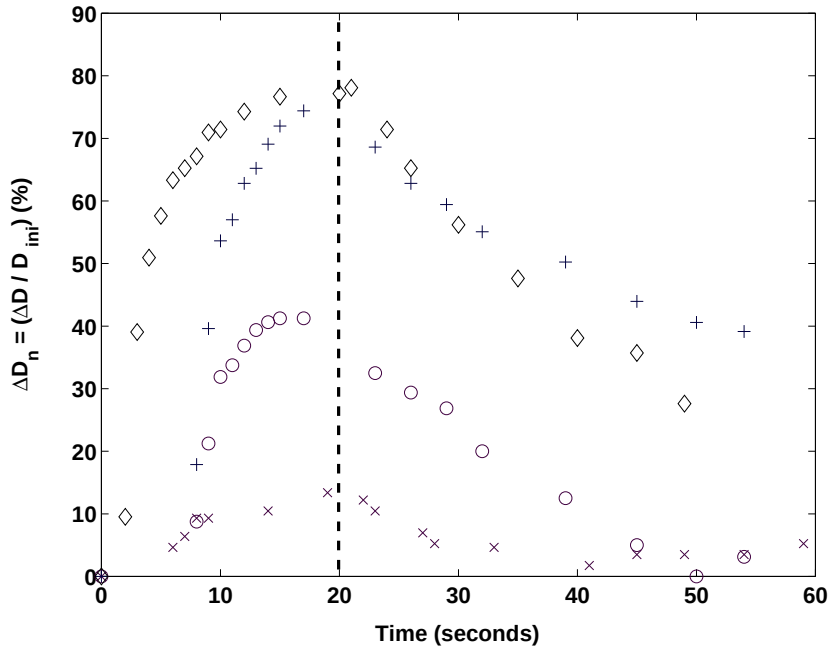

Figure 7.7: Variation of the diameter of nematic domains as a function of time in epifluorescence and reflection mode. The ΔD_n is computed by taking the ratio of the difference between the final diameter, D_f, and the initial diameter, D_{ini}, to the D_{ini} and is expressed in percentage. Here, the domains were illuminated under epifluorescence mode in the first 20 seconds(indicated by dashed line) and switched over to reflection mode after 20 seconds.

We have also observed the textures of nematic domains which are birefringent under polarising microscope at A-W interface. In this experiment, we have used the Hg lamp(100 W) as a source in the transmission mode and the halogen lamp in the reflection mode. The nematic domains which was placed between the crossed polaroids, were illuminated with white light(Hg lamp). The intensity of the beam was controlled using a diaphragm. Initially, the domain diameter increased with the increase in intensity. Under polarising setup, a four brush Schlieren texture was seen. On continuing the illumination there was a perturbation in the four brush defect pattern. This is due to the heating of the domains. This is shown in Figure 7.9. For a bigger domain under polarising microscope, we observe the melting of the defect pattern as a function of time. Finally, the pattern vanishes indicating an nematic to isotropic transition. This sequence of melting is shown in the Figure 7.10. We have carried out the effect of illumination under epifluorescence on a dye doped 6CB liquid crystal domains which exhibits isotropic phase at on the A-W interface at room temperature. We

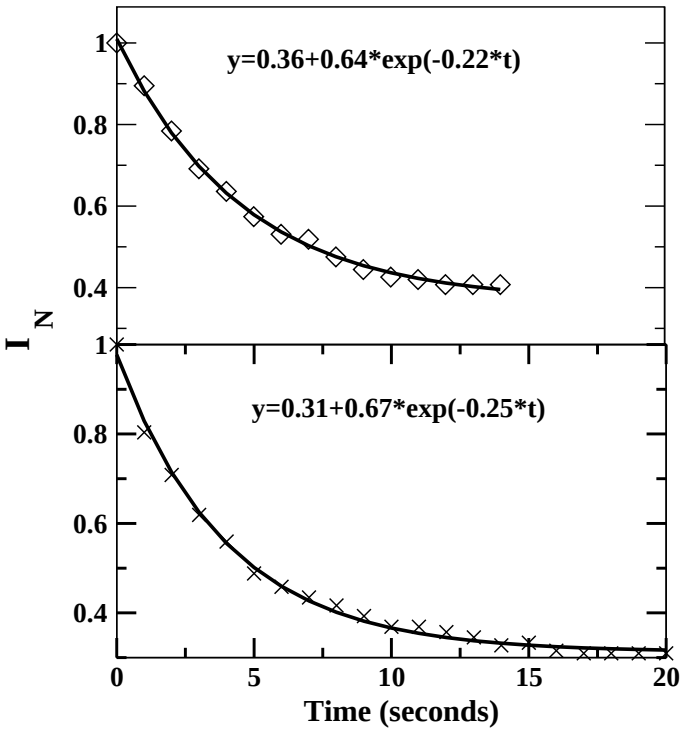

Figure 7.8: Variation of the fluorescent intensity, I_N determined from the grey scale values from images of nematic domains as a function of time for two different nematic domains. The symbols gives the experimental value and the continuous lines give the least square fit.

find that on illumination, there is a slight increase in diameter which was not as significant as that of nematic domain.

An evolution of flat pyramidal shaped domains with terrace structure(multilayer) was proposed by de Gennes and Cazabat [26]. In their model, the following assumptions were made. The molecules from the 2D incompressible fluid in each terrace permeates from the upper terrace to the lower terrace only in a thin annulus at the borders of each terrace. This motion was complicated and coupled between the terraces. Here, the time scale was too long(few days).

In free standing films, surface tension gradient induced flow has been reported [27]. Recently, theoretical studies on Marangoni flow in nematic isotropic interfaces has been reported to exhibit surface tension driven flow caused by tangential stresses that appear due to tangential surface gradients [28]. Also, the orientation of the director from the easy axis of an isotropic fluid−nematic interface led to orientation induced Marangoni effect [29]. We

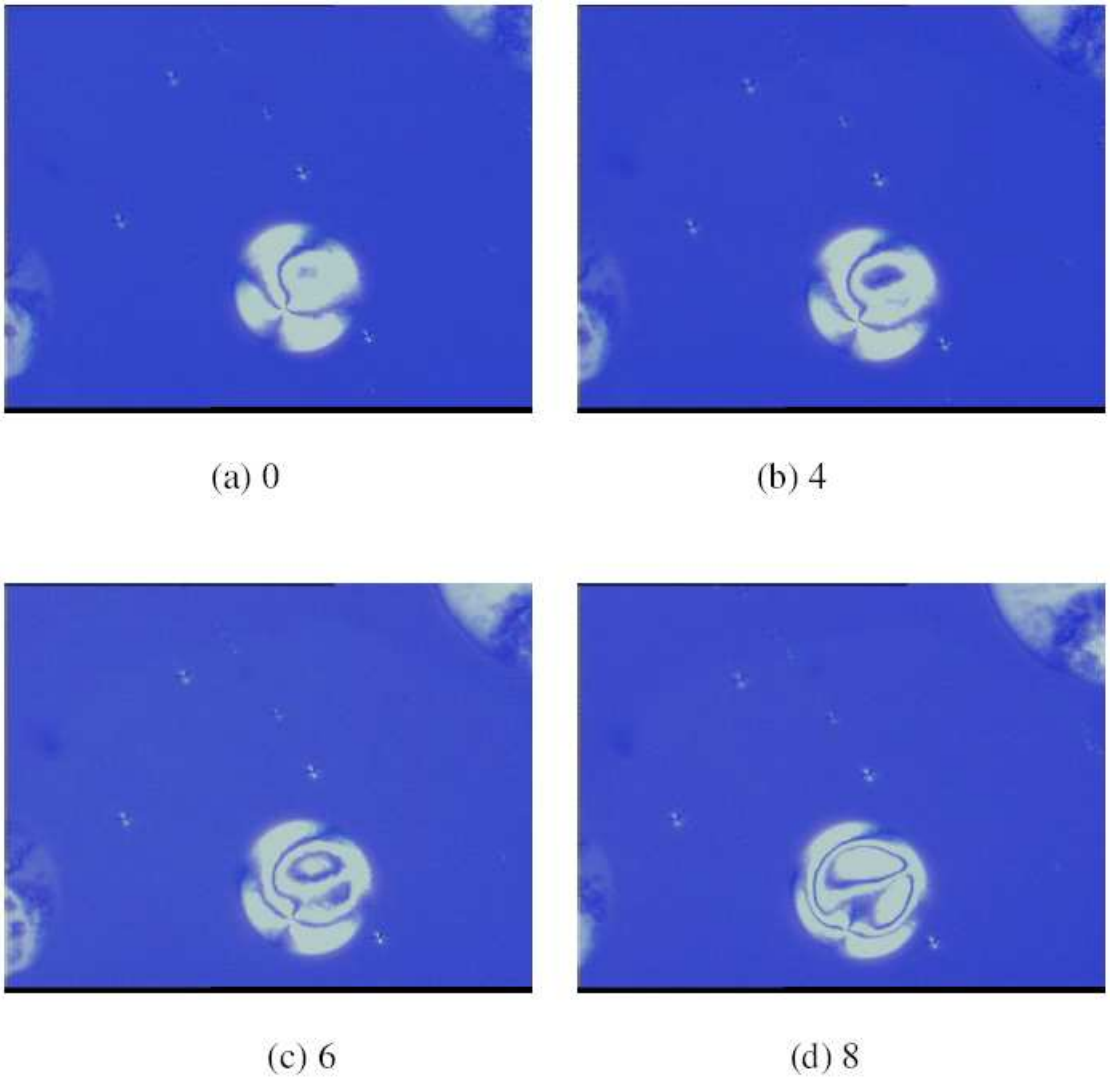

Figure 7.9: Polarising microscope images of nematic domains. Figures (a) to (d) show the nematic domains upon increasing intensity, perturbs the director orientation resulting in change in the texture. The time in seconds are given below each image. Scale of each image is 470 x 350 μm^2.

attribute the wetting nature of the LC domains to the surface tension gradient caused by the photo bleached impurities resulting in concentration gradient($d\gamma_{(LC-air)}/dc$) across the liquid crystal domains. It is quite possible that the fluorescent dye which absorbs during excitation gets locally heated up. This sets up a temperature gradient($d\gamma_{(LC-air)}/dT$) across the LC domains. The net surface tension gradient gives rise to Marangoni effect resulting in flow of material within the LC domains changing its size and thickness. This is supported by our epifluorescence microscopy observations when we see the movement of layers(Figures

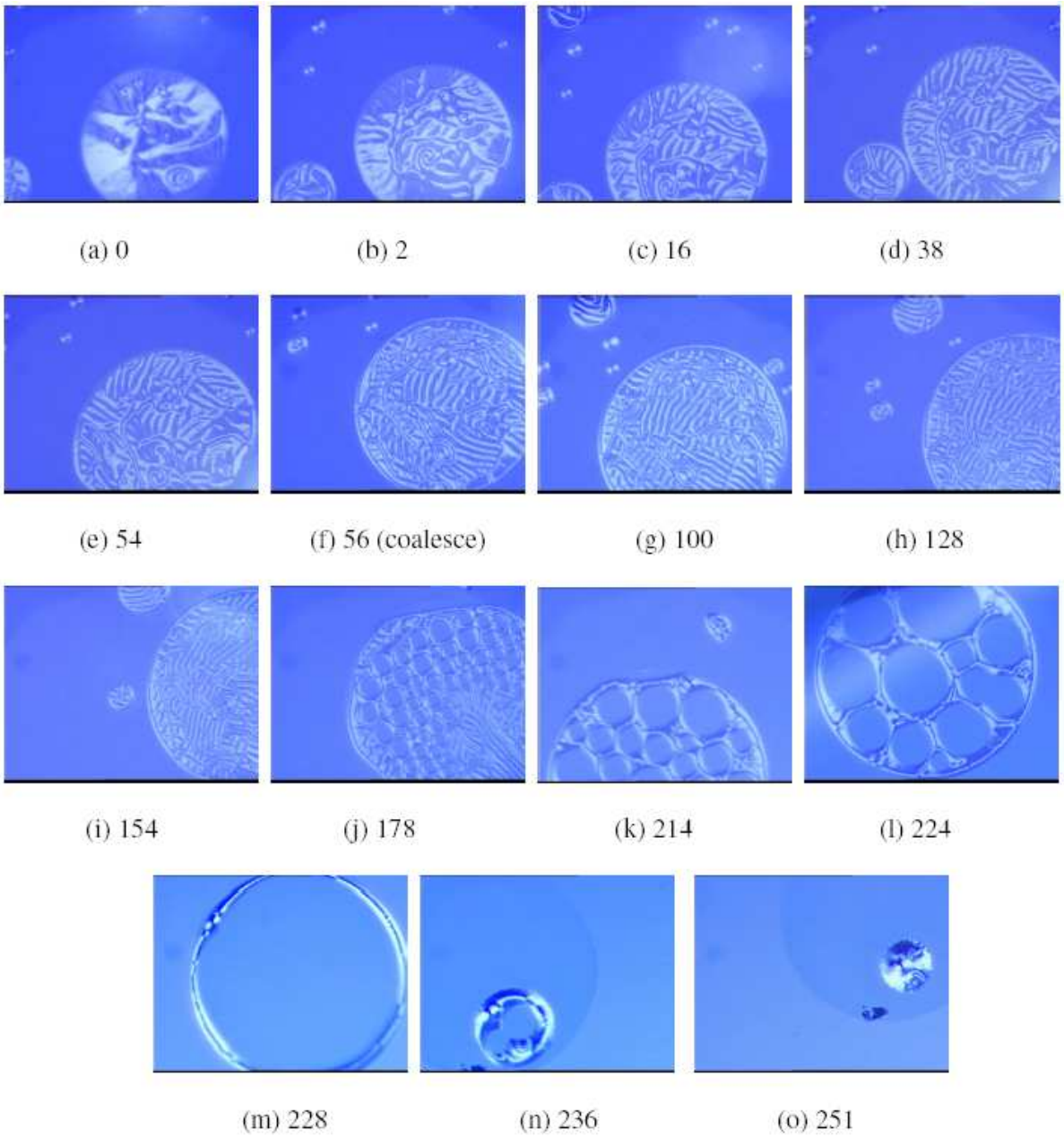

Figure 7.10: Polarising microscope images of nematic domain. Figures (a) to (o) show the melting sequence for nematic domain. Here, the domains undergo a nematic to isotropic phase transition due to heating caused by intense light from the Hg lamp. The birefringent textures tend to melt during illumination and the pattern vanishes. The time in seconds are given below each image. Scale of each image is 470 x 350 μm^2.

7.3(d) to 7.3(g)). The liquid in a domain is pulled towards the regions of higher surface tension. The periphery of the spreading domain when contaminated by the impurities, led to a considerable increase of the spreading rate. Also a significant contribution from diffusion of the photo bleached impurity and the fluorescent dye can't also be ruled out [30].

A pattern formation of the monolayer in the liquid condensed phase at A-W interface has been reported [31]. This pattern formation was driven by the surface tension gradient since the temperature within the field of view is higher than the surrounding regions. Here, the heating is due the source itself causing a temperature difference. The resulting surface tension gradient transports molecules continuously into the field of view changed the morphology of domains in the liquid condensed phase in the monolayer.

To summarize, we have found a novel way to create the surface tension gradient in thin liquid crystal domains. Our results indicate, that for smectic domains, this leads to asymmetric flow resulting in the decrease of thickness and increase in diameter during excitation. Under reflection, this was reversible when the liquid crystal was doped with low dye concentration. However if the dye concentration was more the deformation was permanent. We find a coupling between the layers during flow. For nematic, there was an uniform increase in diameter during photobleaching and was reversible under reflection. In general, if the liquid crystal was photobleached for the first time, then this effect was more prominent when compared to repeated bleaching. This can be understood as due to the depletion of the fluorescent molecules.

Bibliography

[1] P.G. de Gennes, Rev. Mod. Phys., **57**, 827, 1985.

[2] B.Jerome, Rep. Prog. Phys., **54**, 391, 1991.

[3] P.G. de Gennes and A.M. Cazabat, Course 6 and course 8 in *Les Houches session XLVIII - Liquids at interfaces*, Edited by, J. Charvolin, J.F. Joanny and J. Zinn-justin:North Holland, Elsevier Science Publishers, 1990.

[4] K.A. Suresh, Y. Shi, A. Bhattacharyya and S. Kumar, **15**, 225, 2001.

[5] H.W. Hardy, Phil. Mag., **38**, 49, 1919.

[6] F. Vandenbrouck, S. Bardon, M.P. Valignat and A.M. Cazabat, Phys. Rev. Lett., **81**, 610, 1998.

[7] S. Bardon, R. Ober, M.P. Valignat, F. Vandenbrouck, A.M. Cazabat and J. Daillant, Phys. Rev. E., **59**, 6808, 1999.

[8] S. Bardon, M.P. Valignat, A.M. Cazabat, W. Stocker and J.P. Rabe, Langmuir, **14**, 2916, 1998.

[9] L. Xu, M. Salmeron and S. Bardon, Phys. Rev. Lett., **84**, 1519, 2000.

[10] V.G. Levich, *Physicochemical Hydrodynamics*, Prentice Hall:N.J., 1962.

[11] D.A. Edwards, H. Brenner and D.T. Wasan, *Interfacial Transport Processes and Rheology*, Butterworth:MA., 1991.

[12] L.E. Scriven and C.V. Sternling, Nature, **187**, 186, 1960.

[13] *Soft Matter Physics*, Edited by Daoud and Williams, Springer-Verlag:1999.

[14] H.A. Stone and L.G. Leal, Jour. Fluid Mech., **220**, 161, 1990.

[15] W.J. Milliken, H.A. Stone and L.G. Leal, Phys. Fluids A, **5**, 69, 1993.

[16] Y. Pawar and K.J. Stebe, Phys. Fluids, **8**, 1738, 1996.

[17] C.D. Eggleton, Y.P. Pawar and K.J. Stebe, Jour. Fluid Mech., **385**, 79, 1999.

[18] Y.T. Hu and A. Lips, Phys. Rev. Lett., **91**, 044501, 2003.

[19] F.D.D. Santos and T. Ondarcuhu, Phys. Rev. Lett., **75**, 2972, 1995.

[20] H. Haidara, L. Vonna and J. Schultz, Jour. Chem. Phys., **107**, 630, 1997.

[21] N.V. Madhusudana and K.R. Sumathy, Mol. Crys. Liq. Crys., **92**, 193, 1983.

[22] K.A. Suresh and A. Bhattacharyya, Langmuir, **3**, 1377, 1997.

[23] F. Picano, P. Oswald and E. Kats, Phys. Rev. E., **63**, 021705, 2001.

[24] J. Geminard, R. Holyst and P. Oswald, Phys. Rev. Lett., **78**, 1924, 1997.

[25] S. Pankratz, P.M. Johnson, A. Paulson and C.C. Huang, Phys. Rev. E., **61**, 6689, 2001.

[26] P.G. de Gennes and A.M. Cazabat, C. R. Acad. Sci., Ser. II: Mec. Phys., Chim., Sci. Terre Univers, **310**, 1601, 1990.

[27] M.I. Godfrey and D.H.V. Winkle, Phys. Rev. E., **54**, 3752, 1996.

[28] A.D. Rey, Jour. Chem. Phys., **110**, 9769, 1999.

[29] A.D. Rey, Liquid Crystals, **26**, 913, 1999.

[30] M. Nollmann, D. Shalom, P. Etchegoin and J. Sereni, Phys. Rev. E., **59**, 1850, 1999.

[31] M. Wang, G. Wildburg, J.H. van Esch, P. Bennema, R.J.M. Nolte and H. Ringsdorf, Phys. Rev. Lett., **71**, 4003, 1993.